Accurate Feeding of Nanoantenna by Singular Optics for Nanoscale Translational and Rotational Displacement Sensing

Xi, Zheng; Wei, Lei; Adam, Aurele; Urbach, Paul; Du, L

Important note
To cite this publication, please use the final published version (if applicable).
Please check the document version above.

P H Y S I C A L   R E V I E W   L E T T E R S

Accurate Feeding of Nanoantenna by Singular Optics for Nanoscale Translational and Rotational Displacement Sensing

Zheng Xi,[*] Lei Wei, A. J. L. Adam, and H. P. Urbach

Optics Research Group, Delft University of Technology, Department of Imaging Physics,
Lorentzweg 1, 2628CJ Delft, The Netherlands

Luping Du

Nanophotonics Research Center, Shenzhen University, Nanshan District, Shenzhen, China

Identifying subwavelength objects and displacements is of crucial importance in optical nanometrology. We show in this Letter that nanoantennas with subwavelength structures can be excited precisely by incident beams with singularity. This accurate feeding beyond the diffraction limit can lead to dynamic control of the unidirectional scattering in the far field. The combination of the field discontinuity of the incoming singular beam with the rapid phase variation near the antenna leads to remarkable sensitivity of the far-field scattering to the displacement at a scale much smaller than the wavelength. This Letter introduces a far-field deep subwavelength position detection method based on the interaction of singular optics with nanoantennas.

Great efficiencies have been achieved using nanoantennas to control light at the nanoscale [1–4]. The recently developed configuration of antenna arrays at optical frequencies, also called a metasurface, has propelled many applications of controlling the direction of far-field scattering [5–9]. The dynamic control of the scattering directivity requires precise excitation of the appropriate currents in the antenna [10,11]. Since the building blocks of ultracompact nanoantennas are subwavelength nanoparticles whose size and interparticle gaps are both beyond the diffraction limit, it is quite challenging to distinguish and precisely excite these arrays using far-field optical schemes. Previous works addressed this issue using polarization selective excitation of different antenna elements [6,12]. These antenna arrays are based on a similar concept as those used in microwave antenna arrays, in particular, the gaps between the individual elements are comparable to the working wavelength. One of the promising approaches is to use spatially inhomogeneous light to control the near-field hot spot produced by the nanoantennas [13]. However, it still remains an open question how to precisely excite deep subwavelength antennas for the active control of the far-field unidirectional scattering.

Singular optics has been an intriguing candidate for the study of techniques far beyond the diffraction limit [14]. The singularity usually refers to the discontinuity or undefined value in the light field itself. Around these singularities of the fields, rapidly spatially varying field patterns occur, which has led to new applications such as high-precision nanoscale metrology and superresolution imaging [13,15–23].

In this Letter, we use two different kinds of singularities: The so-called V-point polarization singularity in an

azimuthally polarized beam [24–26] and the phase singularity in a Hermite-Gaussian beam to precisely excite one individual element of two identical parallel metallic nanorod antennas separated by a deep subwavelength gap. The precise alignment of the singularity with the two nanorods gives an accurate feeding of them far beyond the diffraction limit. As will be shown, this excitation mode can be used to dynamically control the unidirectional scattering. More importantly, it is possible to achieve very high resolution in the detection of nanoscale translational and rotational displacements. We show results obtained by rigorous simulations and present a sufficiently accurate model based on two interacting electric dipoles to explain the rapid change of the scattering pattern for subwavelength displacements. In contrast to what may be expected, in the proposed scheme, it is better to use a longer wavelength for the detection of smaller displacements. The detection sensitivity can be further increased by forming arrays of these nanorods.

Let us first consider the case of the focused azimuthally polarized beam shown in Fig. 1(a). The interaction of this beam with nanoantennas has shown great potential in the excitation of dark modes [27] as well as ultrahigh enhancement of the field [28]. The numerical aperture is chosen as $NA = 1.45$ with the surrounding medium having refractive index $n = 1.5$. The focused beam is calculated with the Richard-Wolf diffraction integral [29,30] and implemented into a finite difference time domain simulation for the calculation of the interaction of the beam with the nanorods. The azimuthal polarization in the pupil causes a V-point polarization singularity at the center of the focused spot around which the E field is polarized azimuthally [24] [Fig. 1(b)]. If the singular point of the incident beam is
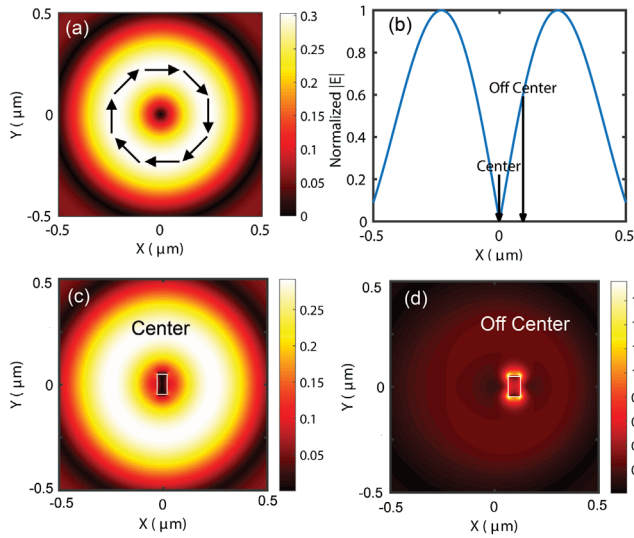
FIG. 1.   (a) Electric field amplitude $|E|$ distribution at the focal plane of a focused azimuthally polarized beam. The black arrows show the direction of polarization. (b) Line cut of $|E|$ through the singularity center. (c) $|E|$ field distribution when a resonant nanorod antenna is placed at the singularity center of the azimuthally polarized beam. (d) $|E|$ field distribution when a resonant nanorod is displaced 100 nm from the singularity center. The gold nanorod has dimensions $50 \times 50 \times 100$ nm^3 shown as the rectangular area. The wavelength is 791 nm. The permittivity of gold is fitted from Ref. [31].

centered on a single gold nanorod, as shown in Fig. 1(c), then due to the symmetry of the field, the induced dipole strength and, hence, the field scattered by the nanorod are small. However, if the nanorod is displaced slightly, the broken symmetry induces a resonant dipole moment inside the nanorod as shown in Fig. 1(d). This position-dependent excitation of the nanorod provides a control mechanism of the scattered radiation and forms the basis for the drastic change of the far-field pattern when two nanorods are considered.

In Fig. 2, we study the configuration when two identical gold nanorods are placed parallel to each other, and the azimuthally polarized beam is focused at the center of the right nanorod shown in Fig. 2(a). The right to left ratio defined as the far-field scattered power in the $+x$ direction divided by that in the $-x$ direction is plotted in Fig. 2(b). A logarithmic scale is used for better illustration. The green and red shaded areas are wavelengths for which the two nanorods scatter more in the $+x$ and the $-x$ directions, respectively. It is seen that the scattering pattern is very sensitive to the wavelength. At the wavelength of 758 nm, the nanorod at the center of the focused beam reflects most of the scattered energy into the $-x$ direction, whereas at wavelengths longer than 840 nm, this antenna directs more power in the $+x$ direction. It is interesting to note that at 840 nm, although the center of the beam is focused at the center of one nanorod resulting in an asymmetric illumination, the far-field scattering pattern is highly symmetric.
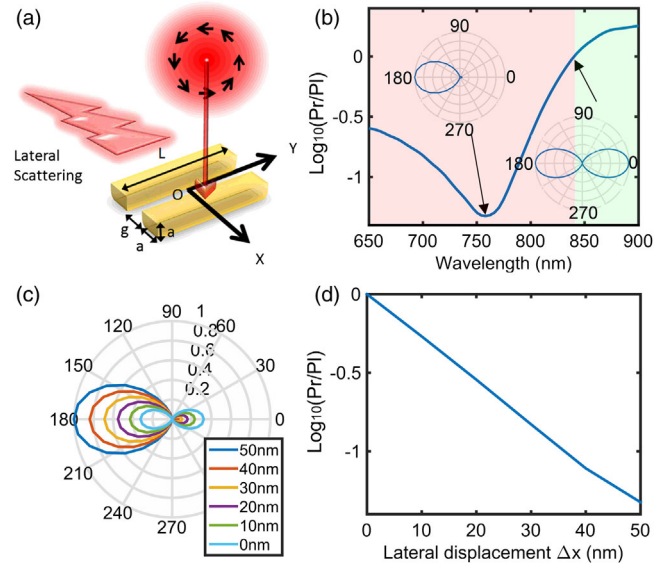
FIG. 2.   (a) Schematic illustration of the considered configuration, the origin of the coordinate system is chosen at the center of the two nanorods. The center of the beam is at the center of the right nanorod. The two nanorods have length $L = 100$ nm and a square cross section with side $a = 50$ nm. The gap between the nanorods is $g = 50$ nm. (b) The ratio of the right ($x > 0$) to left ($x < 0$) scattered power. The insets show the scattering patterns in the XY plane at 758 and 840 nm, respectively. (c) Change of scattering pattern as the singular point is displaced from the origin at the wavelength of 758 nm. (d) Change of right to left scattered power ratio as the singular point is displaced from the origin at the wavelength of 758 nm.

More surprisingly, at 758 nm, when the beam is scanned through the antenna for 50 nm along the $-x$ axis as shown in Fig. 2(c), which is about $0.066\lambda_0$, where λ_0 is the free space wavelength, the scattering pattern changes dramatically from highly asymmetric unidirectional to a symmetric scattering pattern. To quantify this change, in Fig. 2(d), we plot the ratio change as the singular point is moved from the origin for a displacement of 50 nm. The actual ratio changes from 10^0 to $10^{-1.3}$, which is more than one order of magnitude. The drastic change of the far-field scattering pattern results in a remarkable sensitivity to subwavelength displacements. It also provides a way of dynamic control over the far-field scattering pattern by scanning the nanorod, for example, using the piezostage, through the beam center.

A semianalytical theory illustrated in Fig. 3(a) can be applied to explain this phenomenon. The two nanorods are approximated by two point dipoles $\vec{p}_1$ and $\vec{p}_2$ placed at a center-to-center distance $d = g + a$ apart from each other. The phase difference between the two dipoles is $\Delta\Phi$. The illumination fields $\vec{E}_1$ and $\vec{E}_2$ at the center of the two nanorods depend strongly on the lateral displacement. This dipole approximation is considered to be valid as long as the high order multiple resonances in the nanorod are not
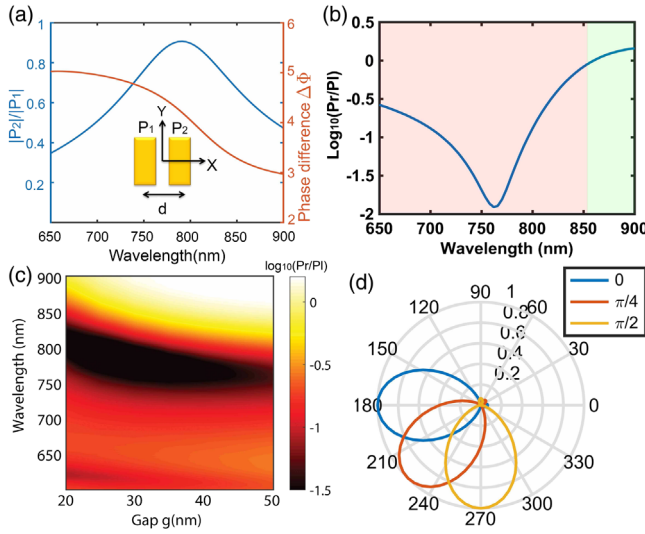
FIG. 3.   (a) Ratio of the strength and phase difference of the two induced dipoles calculated using the semianalytical method. Inset illustrates the model used to describe the unidirectional scattering behavior. Two nanorods are modeled as coupled electric dipoles. (b) Right to left ratio obtained with the semianalytical model. (c) Right to left ratio as a function of wavelength and gap between the nanorods. (d) Rotation of the far-field scattering pattern as the nanorods are rotated over the indicated angles.

excited for the wavelength considered [32]. Interestingly, in some specific systems, the unidirectional scattering can be explained using the interference of a magnetic dipole, an electric dipole, and an electric quadruple [33–37], and there is indeed a magnetic dipole resonance excited in the proposed system. As we will show in the following, the explanation using this two-electric-dipole model [38] is good enough to predict the position-dependent changes in the far-field scattering [39]. Considering the coupling between the two dipoles, $\vec{p}_1$ and $\vec{p}_2$ can be written as

$$\vec{p}_1 = \epsilon_0\epsilon_r\alpha\vec{E}_1 + \epsilon_0\epsilon_r\alpha E_n\vec{p}_2,$$
$$\vec{p}_2 = \epsilon_0\epsilon_r\alpha\vec{E}_2 + \epsilon_0\epsilon_r\alpha E_n\vec{p}_1, \qquad (1)$$

with α being the polarizability of each nanorod along the longer axis and E_n being the coupling term:

$$E_n = -e^{ikd}\frac{1 - ikd - k^2d^2}{4\pi d^3\epsilon_0\epsilon_r}. \qquad (2)$$

Although in general, the coupling term should be a tensor due to the vectorial nature of light. Because of the strong anisotropy in the polarizability of the nanorod, it suffices to consider only the component parallel to the longer axis of the nanorod for the considered wavelengths. The total far-field scattering pattern of the two nanorods can be calculated using the far-field expressions for the radiation of two dipoles. The right to left power ratio can be calculated as [32,40,41]

$$P_r/P_l = \frac{|p_1|^2 + |p_2|^2 + 2|p_1||p_2|\cos(\Delta\Phi - kd)}{|p_1|^2 + |p_2|^2 + 2|p_1||p_2|\cos(\Delta\Phi + kd)}. \qquad (3)$$

When the singular point is focused at the center of the two nanorods, the illumination field $\vec{E}_1 = -\vec{E}_2$ because of the antisymmetric distribution in the illumination polarization. The two induced dipole moments are then

$$\vec{p}_1 = \epsilon_0\epsilon_r\frac{\alpha - \alpha^2 E_n}{1 - \alpha^2 E_n^2}\vec{E}_1,$$
$$\vec{p}_2 = -\epsilon_0\epsilon_r\frac{\alpha - \alpha^2 E_n}{1 - \alpha^2 E_n^2}\vec{E}_1. \qquad (4)$$

The antisymmetric distribution of polarization in the illumination with respect to the singular center induces dipole moments inside the two nanorods of equal strength but with a phase difference of π. According to Eq. (3), the power in the right and left directions is the same, and the scattering pattern is symmetric.

The situation begins to change drastically if the singular point is focused at the center of the right nanorod as shown in Fig. 2(a). In this case, the illumination field $\vec{E}_2 = 0$, and we get

$$\vec{p}_1 = \epsilon_0\epsilon_r\frac{\alpha}{1 - \alpha^2 E_n^2}\vec{E}_1,$$
$$\vec{p}_2 = \epsilon_0\epsilon_r\frac{\alpha^2 E_n}{1 - \alpha^2 E_n^2}\vec{E}_1. \qquad (5)$$

The nanorod $\vec{p}_2$ is hardly excited by the focused beam; it can only be excited by the coupling of the adjacent nanorod $\vec{p}_1$. The phase difference between the two nanorods is no longer determined by the incident beam but instead by the interaction [32]:

$$\vec{p}_2 = \alpha E_n\vec{p}_1$$
$$= -\alpha e^{ikd}(1 - ikd - k^2d^2)/(4\pi\epsilon_r\epsilon_0 d^3)\vec{p}_1. \qquad (6)$$

At very short distance d, the induced dipole $\vec{p}_2$ in the center nanorod varies very sensitively. To determine the phase difference $\Delta\Phi$, the polarizability α is needed. We performed numerical simulations to extract this parameter [39,42]. In Fig. 3(a), we plot the amplitude ratio between the two induced dipoles $\vec{p}_2$ and $\vec{p}_1$ inside the two nanorods and the phase difference $\Delta\Phi$ between them. A clear enhancement of $\vec{p}_2$ due to a plasmonic resonance can be seen. Because of the coupling between the two nanorods, the two induced dipole moments are not equal. Therefore, the condition for maximum right to left ratio $\Delta\Phi = \pi/2$ as implied by Eq. (3) when $|\vec{p}_1| = |\vec{p}_2|$ is no longer valid. In Fig. 3(b), we plot the right to left ratio calculated using the semianalytical method. Good agreement is obtained with the results obtained by rigorous numerical computations shown in Fig. 2(b). The mismatch is due to the change of the electric polarizability of the individual nanorod due to strong coupling.

From the discussions above, it follows that the singular point in the azimuthally polarized beam provides a way to accurately control the separate excitations of the two nanorods, even when the gap is deep subwavelengths. We now consider the effect of using smaller gaps. We decrease the gap size $g = d - a$ between the two nanorods from 50 to 20 nm and rigorously compute the right to left ratio in Fig. 3(c). A very strong directivity at 800 nm can still be observed even when the gap g is only 20 nm. Therefore, even for a displacement of 35 nm (about $0.04\lambda_0$), the change from a highly asymmetric pattern to a highly symmetric one can still be observed indicating higher sensitivity using the smaller gap. One interesting thing to note here is that as the gap g between the two nanorods decreases, the wavelength at which the right to left ratio is maximum shifts to a longer wavelength. In contrast to what one may expect, in this case a longer wavelength is better suited for the detection of smaller displacements. The explanation for this surprising phenomenon is the plasmonic resonance of the two nanorods: The phase difference of the two excited dipole moments is determined by the resonant excitation of the two nanorods. As the nanorods approach each other, their resonance shifts to longer wavelengths due to near-field coupling. Although we quantify the displacement in terms of wavelength here, this is actually not a good way of defining the minimum displacement. As we showed above, it is the abrupt polarization change at the beam center along with the rapid change of phase in the near field that lead to the very high sensitivity in the far-field scattering symmetry. The phase in the near field depends strongly on the resonant coupling. The resonance can be shifted to even longer wavelengths when the length of the two nanorods is increased [43], while the detection limit is still determined by the gap size. Therefore, the gap size is a more important limiting factor for the displacement detection than the wavelength used.

When the two nanorods are rotated with respect to the singularity center, this rotation can be observed by measuring the rotation of the main lobe of far-field scattered power as shown in Fig. 3(d). Because the illumination is rotationally symmetric, as the rotation angle changes from 0 to $\pi/2$, the far-field scattering pattern changes accordingly. This offers a highly sensitive method of detecting small rotations.

Since the nanorods are placed near the singular point, the scattered power is, although detectable, rather weak. A more strongly directional scattering is desired to make the detection easier. To achieve this, an array of nanorod pairs can be applied to restrict the scattered power within a narrow angular range. The array has the additional advantage that it also collects a larger part of the incident beam. As an example, we apply an array of five nanorod pairs parallel to the y direction which we illuminate with a Hermite-Gaussian beam with a singular line as shown in Figs. 4(a) and 4(b). The polarization of the incident beam is parallel to the y direction. The pitch along the y direction is chosen as 253 nm to achieve maximum lateral scattering
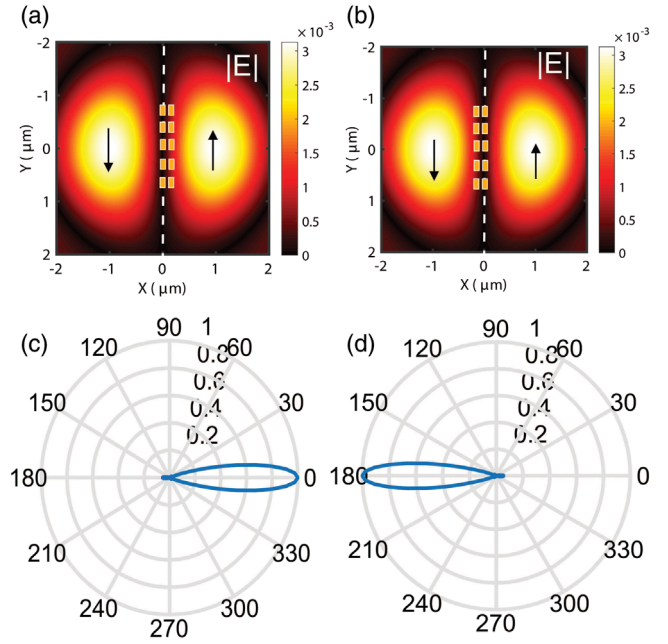

FIG. 4.   (a),(b) Configuration of precise alignment of the arrays with respect to the Hermite-Gaussian beam with a dark singular line (dash line) in the middle. The polarization is along the y direction indicated by the black arrow. The array is shown as gold rectangles. The wavelength is 758 nm with the gap $g = 50$ nm, and the pitch along the y direction is 253 nm. For (a), the dark line is aligned to the left side of the antenna array, while for (b), it is aligned to the right. (c),(d) The far-field scattering pattern in the XY plane of the arrays corresponding to different alignment of the dark line to the left (c) and to the right (d) of the array.

based on the array multiplication principle [44]. The angular scattering pattern is now much narrower, and this further increases the sensitivity of the present scheme as shown in Figs. 4(c) and 4(d).

Finally, we would like to discuss the theoretical detection limit of the present scheme. As shown in the previous discussion, the size of the gap between the two nanorods is an important parameter. However, if the gap is of the order of a few angstroms or less, electrons will start to tunnel from one nanorod to the other [45], implying that the two nanorods get electrically connected, and thus the required phase difference cannot be met. It is worth noting here that the focusing of the beam itself is not a necessity, but by focusing the beam, the power can be more concentrated on the nanorods; therefore, the detected scattering power is increased. We have calculated the scattering cross section according to the definition in Ref. [46]. For the single antenna case, the scattering cross section is comparable to experimentally measured values [47], and the detailed value can be found in the Supplemental Material [39].

In summary, we are not only proposing a scheme to control the scattering directionality of the antenna but also a far-field scheme for the detection of the deep subwavelength displacement, which is very important, for example, in overlay alignment in semiconductor industry. The scheme is based on

the interaction of singular optics with metallic resonant optical antennas which brings together several important areas of research: singular optics, vectorial focal field shaping, resonant nanoscale metallic antenna, as well as subwavelength nanometrology into one novel research direction. We note the physics relies on the symmetry of the excitation and the antenna structure, as well as the resonant responses of the antenna. In general, the resonances can also come from other modes. Although our work is based on metallic nanoantennas, the working principles can be applied for dielectric nanoantennas as well. With the introduction of a singular beam with a resonant optical antenna, a new degree of freedom can be brought into the area of detection of deep subwavelength displacements.

*z.xi@tudelft.nl

[1] L. Novotny and N. Van Hulst, Nat. Photonics **5**, 83 (2011).
[2] P. Bharadwaj, B. Deutsch, and L. Novotny, Adv. Opt. Photonics **1**, 438 (2009).
[3] A. G. Curto, G. Volpe, T. H. Taminiau, M. P. Kreuzer, R. Quidant, and N. F. van Hulst, Science **329**, 930 (2010).
[4] A. G. Curto, T. H. Taminiau, G. Volpe, M. P. Kreuzer, R. Quidant, and N. F. van Hulst, Nat. Commun. **4**, 1750 (2013).
[5] K. Bliokh, F. Rodríguez-Fortuño, F. Nori, and A. Zayats, Nat. Photonics **9**, 796 (2015).
[6] J. Lin, J. B. Mueller, Q. Wang, G. Yuan, N. Antoniou, X.-C. Yuan, and F. Capasso, Science **340**, 331 (2013).
[7] N. Yu, P. Genevet, M. A. Kats, F. Aieta, J.-P. Tetienne, F. Capasso, and Z. Gaburro, Science **334**, 333 (2011).
[8] N. Yu and F. Capasso, Nat. Mater. **13**, 139 (2014).
[9] L. Liu, X. Zhang, M. Kenney, X. Su, N. Xu, C. Ouyang, Y. Shi, J. Han, W. Zhang, and S. Zhang, Adv. Mater. **26**, 5031 (2014).
[10] Z. Xi, L. Wei, A. J. L. Adam, and H. P. Urbach, Opt. Lett. **41**, 33 (2016).
[11] L. Wei, Z. Xi, N. Bhattacharya, and H. P. Urbach, Optica **3**, 799 (2016).
[12] K. Lindfors, D. Dregely, M. Lippitz, N. Engheta, M. Totzeck, and H. Giessen, ACS Photonics **3**, 286 (2016).
[13] G. Volpe, S. Cherukulappurath, R. Juanola Parramon, G. Molina-Terriza, and R. Quidant, Nano Lett. **9**, 3608 (2009).
[14] M. R. Dennis, K. O'Holleran, and M. J. Padgett, Prog. Opt. **53**, 293 (2009).
[15] S. W. Hell, R. Schmidt, and A. Egner, Nat. Photonics **3**, 381 (2009).
[16] J. Fischer and M. Wegener, Laser Photonics Rev. **7**, 22 (2013).
[17] J. Shamir, Opt. Eng. (Bellingham, Wash.) **51**, 073605 (2012).
[18] S. Roy, K. Ushakova, Q. van den Berg, S. F. Pereira, and H. P. Urbach, Phys. Rev. Lett. **114**, 103903 (2015).
[19] M. Neugebauer, P. Woźniak, A. Bag, G. Leuchs, and P. Banzer, arXiv:1511.02066.

[20] O. G. Rodríguez-Herrera, D. Lara, K. Y. Bliokh, E. A. Ostrovskaya, and C. Dainty, Phys. Rev. Lett. **104**, 253601 (2010).
[21] M. Neugebauer, T. Bauer, A. Aiello, and P. Banzer, Phys. Rev. Lett. **114**, 063901 (2015).
[22] M. Neugebauer, T. Bauer, P. Banzer, and G. Leuchs, Nano Lett. **14**, 2546 (2014).
[23] T. Bauer, S. Orlov, U. Peschel, P. Banzer, and G. Leuchs, Nat. Photonics **8**, 23 (2014).
[24] I. Freund, Opt. Commun. **201**, 251 (2002).
[25] Y. F. Chen, T.-H. Lu, and K. F. Huang, Phys. Rev. Lett. **97**, 233903 (2006).
[26] G. Milione, H. I. Sztul, D. A. Nolan, and R. R. Alfano, Phys. Rev. Lett. **107**, 053601 (2011).
[27] M. Hentschel, J. Dorfmüller, H. Giessen, S. Jäger, A. M. Kern, K. Braun, D. Zhang, and A. J. Meixner, Beilstein J. Nanotechnol. **4**, 57 (2013).
[28] J. Scheuer, Opt. Express **19**, 25454 (2011).
[29] E. Wolf, Proc. R. Soc. A **253**, 349 (1959).
[30] B. Richards and E. Wolf, Proc. R. Soc. A **253**, 358 (1959).
[31] P. B. Johnson and R.-W. Christy, Phys. Rev. B **6**, 4370 (1972).
[32] B. Rolly, B. Stout, S. Bidault, and N. Bonod, Opt. Lett. **36**, 3368 (2011).
[33] S. R. K. Rodriguez, F. B. Arango, T. P. Steinbusch, M. A. Verschuuren, A. F. Koenderink, and J. G. Rivas, Phys. Rev. Lett. **113**, 247401 (2014).
[34] J. Yan, P. Liu, Z. Lin, H. Wang, H. Chen, C. Wang, and G. Yang, ACS Nano **9**, 2968 (2015).
[35] M. V. Rybin, P. V. Kapitanova, D. S. Filonov, A. P. Slobozhanyuk, P. A. Belov, Y. S. Kivshar, and M. F. Limonov, Phys. Rev. B **88**, 205106 (2013).
[36] D. Sikdar, W. Cheng, and M. Premaratne, J. Appl. Phys. **117**, 083101 (2015).
[37] C. Wang, Z. Jia, K. Zhang, Y. Zhou, R. Fan, X. Xiong, and R. Peng, J. Appl. Phys. **115**, 244312 (2014).
[38] T. Pakizeh and M. Käll, Nano Lett. **9**, 2343 (2009).
[39] See the Supplemental Material at http://link.aps.org/supplemental/10.1103/PhysRevLett.117.113903 for the calculation of the polarizability of a single nanorod, scattering cross section under focused beam illumination and the validity of the two-electric-dipole model.
[40] D. Vercruysse, Y. Sonnefraud, N. Verellen, F. B. Fuchs, G. Di Martino, L. Lagae, V. V. Moshchalkov, S. A. Maier, and P. Van Dorpe, Nano Lett. **13**, 3843 (2013).
[41] Z. Xi, Y. Lu, W. Yu, P. Yao, P. Wang, and H. Ming, Opt. Express **21**, 29365 (2013).
[42] E. Poutrina and A. Urbas, J. Opt. **16**, 114005 (2014).
[43] A. M. Funston, C. Novo, T. J. Davis, and P. Mulvaney, Nano Lett. **9**, 1651 (2009).
[44] J. D. Kraus and R. J. Marhefka, Antennas for All Applications (McGraw-Hill, New York, 2002).
[45] K. J. Savage, M. M. Hawkeye, R. Esteban, A. G. Borisov, J. Aizpurua, and J. J. Baumberg, Nature (London) **491**, 574 (2012).
[46] N. M. Mojarad, V. Sandoghdar, and M. Agio, J. Opt. Soc. Am. B **25**, 651 (2008).
[47] M. Husnik, S. Linden, R. Diehl, J. Niegemann, K. Busch, and M. Wegener, Phys. Rev. Lett. **109**, 233902 (2012).